

Contribution from the Department of Chemistry, State University of New York, Stony Brook, New York 11794, and Faculty of Chemistry, Adam Mickiewicz University, Poznan, Poland

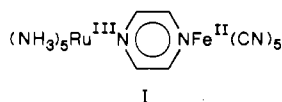
Formation and Properties of the Binuclear Complex $(\text{NH}_3)_5\text{Ru}^{\text{III}}\text{NCFe}^{\text{II}}(\text{CN})_5^-$

Andrzej Burewicz and Albert Haim*

Received October 27, 1987

The kinetics of the title reaction was studied under anaerobic conditions at 25 °C, ionic strength 0.10 M (sodium perchlorate), and pH 4.00–5.32. A catalytic pathway associated with $\text{Ru}(\text{NH}_3)_5\text{OH}_2^{2+}$ produced in the outer-sphere redox equilibration between $\text{Ru}(\text{NH}_3)_5\text{OH}_2^{3+}$ and $\text{Fe}(\text{CN})_6^{4-}$ was suppressed by the addition of $\text{Fe}(\text{CN})_6^{3-}$. The proposed mechanism features rapid formation of the ion pair $\text{Ru}(\text{NH}_3)_5\text{OH}_2^{3+}[\text{Fe}(\text{CN})_6^{4-}]$ (formation constant $(2.1 \pm 0.6) \times 10^3 \text{ M}^{-1}$) and its subsequent slow reaction ($k = (6.9 \pm 0.7) \times 10^{-4} \text{ s}^{-1}$) to produce $(\text{NH}_3)_5\text{Ru}^{\text{III}}\text{NCFe}^{\text{II}}(\text{CN})_5^-$. The latter compound features an intervalence (metal to metal) band at 980 nm (half-bandwidth 4100 cm^{-1} , molar absorptance $3.0 \times 10^3 \text{ M}^{-1} \text{ cm}^{-1}$). The extent of delocalization in the title compound and related cyano-bridged, heterobinuclear complexes is discussed.

We reported previously¹ our studies of the mixed-valence, pyrazine-bridged, heterobinuclear complex I. For comparison



and in view of our longstanding²⁻⁸ interest in cyano-bridged binuclear complexes, we have carried out some studies with the analogous complex II. Compound II has been briefly mentioned



in the literature.⁹ Considerably more information is available for the ruthenium analogue, compound III.^{10,11} We report herein



our studies on the kinetics of formation of II (and briefly of III) from $\text{Ru}(\text{NH}_3)_5\text{OH}_2^{3+}$ and $\text{Fe}(\text{CN})_6^{4-}$ (and from $\text{Ru}(\text{NH}_3)_5\text{OH}_2^{3+}$ and $\text{Ru}(\text{CN})_6^{4-}$), and we address the question of the valence of the ruthenium and iron centers and the extent of delocalization in compound II.

Experimental Section

Materials. The syntheses of $[\text{Ru}(\text{NH}_3)_5\text{Cl}]\text{Cl}_2$ and of $[\text{Ru}(\text{NH}_3)_5\text{OSO}_2\text{CF}_3](\text{CF}_3\text{SO}_3)_2$ followed the literature procedures.^{12,13} Trifluoromethanesulfonic acid was purified by two distillations under reduced pressure. The purifications of the water, the nitrogen, and the sodium perchlorate were described previously.¹⁴ Sodium hexacyanoferrate(II) decahydrate (Fisher), potassium ferricyanide (Fisher), and potassium hexacyanoruthenate(II) trihydrate (Alfa) were used as received.

Kinetic Measurements. A solution containing the desired concentrations of $\text{Ru}(\text{NH}_3)_5\text{OSO}_2\text{CF}_3^{2+}$, buffer (sodium acetate–acetic acid) and sodium perchlorate was deaerated by flushing with nitrogen. To this solution was added anaerobically the desired amount of a deaerated solution of $\text{Fe}(\text{CN})_6^{4-}$ and $\text{Fe}(\text{CN})_6^{3-}$. The resulting mixture was transferred anaerobically to a spectrophotometric cell, which was then placed in the thermostated cell compartment of a Cary 118 spectrophotometer, and the absorbance at 800 nm was recorded as a function of time. The absorbance vs time analog curves were digitized with a 9864A Hewlett-Packard digitizer, and rate constants were calculated (9820A Hewlett-Packard calculator with digitizer interfaced) from a linear least-squares fit of $\ln(A_\infty - A_t)$ vs t . A_t is the absorbance at time t and A_∞ is a calculated value obtained by an iterative procedure. The data treatment with an adjusted A_∞ was adopted because, in several kinetic runs, precipitation at long times precluded the direct measurement of A_∞ . Whenever A_∞ could be measured, it was found to agree within experimental error with the adjusted A_∞ value. All measurements were carried out at 25 °C and ionic strength 0.10 M.

Physical Measurements. Near-infrared and visible spectra were measured with a Cary 17 spectrophotometer. pH measurements were made with a Model 26 Radiometer pH meter.

Results and Discussion

Upon dissolution of $[\text{Ru}(\text{NH}_3)_5\text{OSO}_2\text{CF}_3](\text{CF}_3\text{SO}_3)_2$ in aqueous buffers with pH in the 4–6 range, the solutions initially

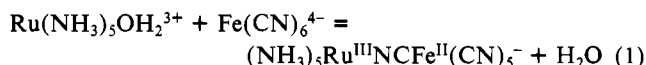
Table I. Kinetics of Formation of $(\text{NH}_3)_5\text{Ru}^{\text{III}}\text{NCFe}^{\text{II}}(\text{CN})_5^-$ ^a

$10^3[\text{Fe}(\text{CN})_6^{3-}]$, M	$10^4 k_{\text{obsd}}$, s^{-1}	$10^3[\text{Fe}(\text{CN})_6^{3-}]$, M	$10^4 k_{\text{obsd}}$, s^{-1}
	3.31	0.975	2.47
0.123	2.45	1.93	2.73
0.497	2.53	2.92	3.41

^a At 25 °C, ionic strength 0.10 M maintained with sodium perchlorate, pH 4.60–4.66, $[\text{Fe}(\text{CN})_6^{4-}] = (1.40\text{--}1.44) \times 10^{-3} \text{ M}$, $[\text{Ru}(\text{NH}_3)_5\text{OH}_2^{3+}] + [\text{Ru}(\text{NH}_3)_5\text{OH}_2^{2+}] = (4.6\text{--}4.9) \times 10^{-5} \text{ M}$.

contain the ion $\text{Ru}(\text{NH}_3)_5\text{OSO}_2\text{CF}_3^{2+}$. However, within about 5 min (rate constant for aquation at 25 °C is $1.9 \times 10^{-2} \text{ s}^{-1}$),¹³ the CF_3SO_3^- ligand is quantitatively replaced by water. In all measurements, the ruthenium solutions were kept for at least 10 min; therefore, in all studies we are dealing with $\text{Ru}(\text{NH}_3)_5\text{OH}_2^{3+}$ and its conjugate base $\text{Ru}(\text{NH}_3)_5\text{OH}_2^{2+}$ (the $\text{p}K_a$ of $\text{Ru}(\text{NH}_3)_5\text{OH}_2^{3+}$ is 4.1¹⁵).

When $\sim 5 \times 10^{-5} \text{ M}$ solutions of $\text{Ru}(\text{NH}_3)_5\text{OH}_2^{3+}/\text{Ru}(\text{NH}_3)_5\text{OH}_2^{2+}$ at pH 4.6 are treated with $(1\text{--}5) \times 10^{-3} \text{ M}$ $\text{Fe}(\text{CN})_6^{4-}$ without exclusion of air, a green color develops over a period of hours. When dioxygen is precluded, a blue color develops. In quantitative terms, in the presence of dioxygen, absorption maxima develop at 980 and 420 nm. Even after the 980-nm maximum ceases growing, the 420-nm maximum continues increasing in absorbance. In the absence of dioxygen, only the 980-nm maximum develops. The 420-nm maximum is characteristic⁵ of $\text{Fe}(\text{CN})_6^{3-}$. Evidently, in the presence of dioxygen oxidation of $\text{Fe}(\text{CN})_6^{4-}$ to $\text{Fe}(\text{CN})_6^{3-}$ occurs, whereas no such oxidation obtains when dioxygen is precluded.¹⁶ The 980-nm maximum corresponds to the intervalence (IV, metal to metal charge transfer) band of II, which is generated according to eq 1.

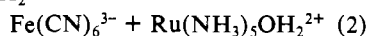


The kinetics of reaction 1 was measured by following the absorbance increase at 800 nm associated with the formation of II. All measurements were carried out in the absence of dioxygen at 25 °C and ionic strength 0.10 M with a large excess of Fe

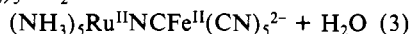
- Yeh, A.; Haim, A. *J. Am. Chem. Soc.* **1985**, *107*, 369.
- Haim, A.; Wilmarth, W. K. *J. Am. Chem. Soc.* **1961**, *83*, 509.
- Egen, N. B.; Castello, R.; Piriz-MacColl, C. *Inorg. Chem.* **1969**, *8*, 699.
- Castello, R.; Piriz-MacColl, C.; Haim, A. *Inorg. Chem.* **1971**, *10*, 203.
- Rosenhein, L.; Haim, A. *Inorg. Chem.* **1974**, *13*, 1571.
- Speer, L. O.; Gaswick, D.; Haim, A. *J. Am. Chem. Soc.* **1977**, *99*, 7894.
- Gaswick, D.; Haim, A. *J. Inorg. Nucl. Chem.* **1978**, *40*, 437.
- Phillips, J.; Haim, A. *Inorg. Chem.* **1980**, *19*, 1616.
- Ludi, A. *Chimia* **1971**, *26*, 647.
- Vogler, A.; Kisslinger, J. *J. Am. Chem. Soc.* **1982**, *104*, 2311.
- Siddiqui, S.; Henderson, W. W.; Shepherd, R. E. *Inorg. Chem.* **1987**, *26*, 3101.
- Vogt, L. H. Jr.; Katz, J. L.; Wiberley, S. E. *Inorg. Chem.* **1965**, *4*, 1157.
- Dixon, N. E.; Lawrance, G. A.; Lay, P. A.; Sargeson, A. M. *Inorg. Chem.* **1984**, *23*, 2940.
- Szecsny, A. P.; Haim, A. *J. Am. Chem. Soc.* **1981**, *103*, 1679.
- Kuehn, C. G.; Taube, H. *J. Am. Chem. Soc.* **1976**, *98*, 689.
- The oxidation of $\text{Fe}(\text{CN})_6^{4-}$ by dioxygen appears to be accelerated by the presence of $\text{Ru}(\text{NH}_3)_5\text{OH}_2^{3+}/\text{Ru}(\text{NH}_3)_5\text{OH}_2^{2+}$ and/or II.

* To whom correspondence should be addressed at the State University of New York.

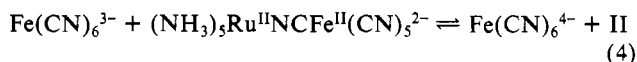
(CN)₆⁴⁻ over Ru(NH₃)₅OH₂³⁺/Ru(NH₃)₅OH₂²⁺. It is well-known¹⁷ that Ru(NH₃)₅OH₂³⁺ catalyzes the equilibration of Ru(NH₃)₅OH₂³⁺ + ligand systems. Therefore, we anticipated that the Ru(NH₃)₅OH₂³⁺-Fe(CN)₆⁴⁻ reaction would be susceptible to such catalysis since the rapid outer-sphere reaction between Fe(CN)₆⁴⁻ and Ru(NH₃)₅OH₂³⁺, eq 2, would generate the sub-



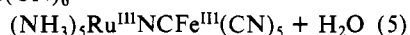
stitution-labile species Ru(NH₃)₅OH₂²⁺. The latter in turn would react rapidly with Fe(CN)₆⁴⁻, eq 3, and finally II would be produced by the rapid outer-sphere redox reaction, eq 4. Entirely



duced by the rapid outer-sphere redox reaction, eq 4. Entirely



analogous mechanisms have been postulated to account for the unusually rapid substitution of H₂O by I⁻ in *trans*-Ru(NH₃)₄-(isn)OH₂³⁺ (isn = isonicotinamide)¹⁸ and the photocatalyzed substitution of Cl⁻ in Ru(NH₃)₅Cl²⁺ by Ru(CN)₆⁴⁻ to produce III.¹⁰ According to the mechanism represented by eq 2-4, the observed rate constant for the catalytic pathway is $k_3K_2[\text{Fe(CN)}_6^{4-}]^2/[\text{Fe(CN)}_6^{3-}]$; e.g., the catalytic reaction would be inhibited by the addition of Fe(CN)₆³⁻. This prediction was tested by carrying out a series of experiments in the presence of added Fe(CN)₆³⁻. The results, summarized in Table I, show that the addition of small amounts of Fe(CN)₆³⁻ decrease the reaction rate and that a constant rate is reached with $[\text{Fe(CN)}_6^{3-}] = (1.23-9.75) \times 10^{-4}$ M. However, at substantially higher concentrations ((1.93-2.92) × 10⁻³ M) the reaction rate increases again. The decrease in rate is consistent with a shift of the equilibrium in eq 2 by the addition of Fe(CN)₆³⁻ and the accompanying decrease in the concentration of the postulated catalytic species Ru(NH₃)₅OH₂²⁺. Taking the oxidation potentials of the Fe(CN)₆^{3-/4-} and Ru(NH₃)₅OH₂^{3+/2+} couples as 0.43¹⁹ and 0.10 V,¹⁵ we calculate²⁰ for the first experiment of Table I that $[\text{Ru(NH}_3)_5\text{OH}_2^{2+}] = 4.3 \times 10^{-7}$ M before any formation of II takes place. For the second through the fourth experiments of Table I, the calculated values of $[\text{Ru(NH}_3)_5\text{OH}_2^{2+}]$ are 1.5×10^{-9} , 3.8×10^{-10} and 1.9×10^{-10} M, respectively. The more than 100-fold decrease in the concentration of Ru(NH₃)₅OH₂²⁺ upon addition of modest amounts of Fe(CN)₆³⁻ parallels the sharp decrease in k_{obsd} . It is noteworthy that after complete inhibition of the catalytic pathway is achieved, a substantial reaction rate remains. Such rate represents the intrinsic reactivity of Ru(NH₃)₅OH₂³⁺ toward Fe(CN)₆⁴⁻. At much higher concentrations of Fe(CN)₆³⁻ (which exceed the concentration of Fe(CN)₆⁴⁻) a modest increase in k_{obsd} obtains. Presumably, substitution of Fe(CN)₆³⁻ into Ru(NH₃)₅OH₂³⁺ (eq 5) followed by rapid reduction (eq 6) of the



binuclear complex formed in eq 5 by Fe(CN)₆⁴⁻ provides a new catalytic pathway for the formation of II. On the basis of these observations, all kinetic measurements on the formation of II were carried out in the presence of 2.5×10^{-4} M Fe(CN)₆³⁻, a concentration sufficiently high to inhibit catalysis by Ru(NH₃)₅OH₂²⁺ but too low to provide a significant contribution to the direct reaction with Ru(NH₃)₅OH₂²⁺ (eq 5).

Reaction 1 was studied as a function of $[\text{Fe(CN)}_6^{4-}]$ and of pH. The results, depicted in Figure 1, show that k_{obsd} increases

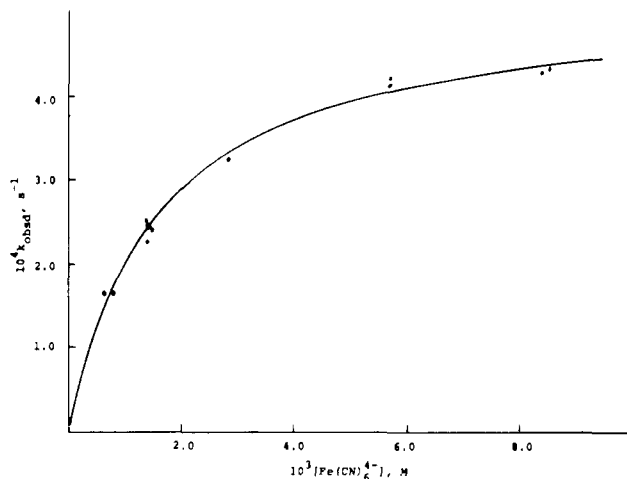


Figure 1. k_{obsd} vs $[\text{Fe(CN)}_6^{4-}]$: points, experimental values; solid line, calculated from eq 9 and the parameters given in the text. Measurements were taken at 25 °C, ionic strength 0.10 M, pH 4.60-4.65, and $[\text{Fe(CN)}_6^{3-}] = 2.5 \times 10^{-4}$ M.

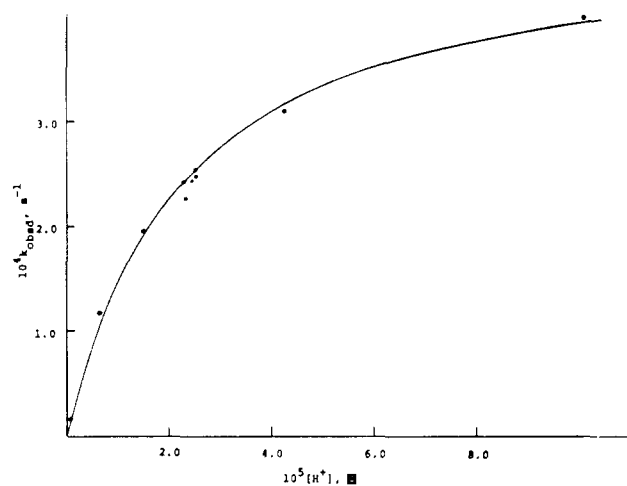
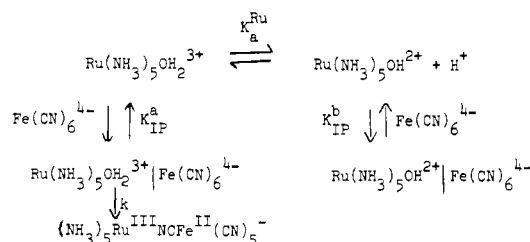
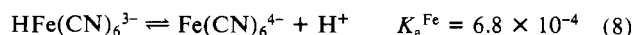
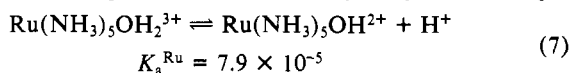


Figure 2. k_{obsd} vs $[\text{H}^+]$: points, experimental values; solid line, calculated from eq 9 and the parameters given in the text. Measurements were taken at 25 °C, ionic strength 0.10 M, $[\text{Fe(CN)}_6^{4-}] = 1.42 \times 10^{-4}$ M, and $[\text{Fe(CN)}_6^{3-}] = 2.5 \times 10^{-4}$ M.

Scheme I



with $[\text{Fe(CN)}_6^{4-}]$ and that a saturation effect obtains at high concentrations. Moreover, it will be seen, as displayed in Figure 2, that k_{obsd} decreases with decreasing $[\text{H}^+]$. In the pH range under study (4.00-5.25), acid-base reactions of the two reactants are important (eq 7 and 8).^{15,21} Cursory²² experiments at pH



(17) Taube, H. *Comments Inorg. Chem.* **1981**, *1*, 17.

(18) Richardson, D. E.; Taube, H. *Inorg. Chem.* **1979**, *18*, 549.

(19) Curtis, J. C.; Meyer, T. J. *Inorg. Chem.* **1982**, *21*, 1562.

(20) Since the concentrations of Ru(NH₃)₅OH₂³⁺ + Ru(NH₃)₅OH₂²⁺ in the experiments reported in Table I cover the range (4.6-4.9) × 10⁻⁵ M, the calculation of $[\text{Ru(NH}_3)_5\text{OH}_2^{2+}]$ is normalized to an initial $[\text{Ru(NH}_3)_5\text{OH}_2^{3+}] = 5.00 \times 10^{-5}$ M.

(21) Jordan, J.; Ewing, C. J. *Inorg. Chem.* **1962**, *1*, 587.

(22) The reaction becomes so slow that several days are necessary for the reaction to proceed to completion. Under these conditions, precipitation of the very insoluble Na[(NH₃)₅RuNCFe(CN)₅] interferes with the absorbance measurements.

Table II. Selected Properties of Intervallence Bands for Cyano-Bridged Binuclear Complexes

complex	10 ⁻⁴ ν _{max} ^a cm ⁻¹	10 ⁻³ ν _{1/2} ^a cm ⁻¹	10 ⁻³ ε, M ⁻¹ cm ⁻¹	10 ² α ^{2b}	10 ⁻³ H _{AB} ^c cm ⁻¹
(NH ₃) ₅ Ru ^{III} NCFe ^{II} (CN) ₅ ⁻	1.02	4.90	3.0	2.2	1.5
(NH ₃) ₅ Ru ^{III} NCRu ^{II} (CN) ₅ ⁻	1.46	5.8	2.8	1.7	1.9
(NH ₃) ₅ Os ^{III} NCFe ^{II} (CN) ₅ ⁻	1.59 ^d	6.05	1.6	0.98	1.5
(NH ₃) ₅ Os ^{III} NCRu ^{II} (CN) ₅ ⁻	2.04 ^d	6.87	2.4	0.97	2.0
(NH ₃) ₅ Os ^{III} NCOs ^{II} (CN) ₅ ⁻	1.79 ^d	6.43	2.1	1.2	1.9
(NH ₃) ₅ Ru ^{III} NCRu ^{II} (bpy) ₂ CN ³⁺	1.44 ^e	5.77	3.5	2.2	2.1

^a Calculated from eq 13. ^b Calculated from eq 11. ^c Calculated from eq 12. ^d From ref 28. ^e From ref 37.

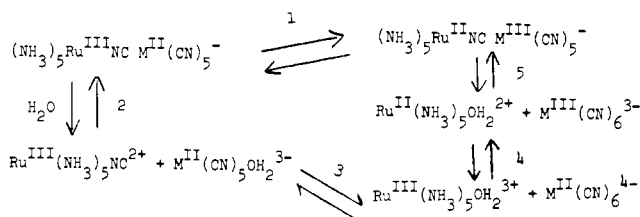
>7 suggest that Ru(NH₃)₅OH²⁺ is unreactive. Therefore, the mechanism depicted in Scheme I is postulated²³ to account for the observed dependences upon [Fe(CN)₆⁴⁻] and [H⁺]. According to Scheme I, the observed rate constant is given by eq 9. Values

$$k_{\text{obsd}} = \frac{[kK_{\text{IP}}^{\text{a}}[\text{H}^+]K_{\text{a}}^{\text{Fe}}[\text{Fe}(\text{CN})_6^{4-}]/([\text{H}^+] + K_{\text{a}}^{\text{Fe}})]/([\text{H}^+] + K_{\text{a}}^{\text{Ru}} + (K_{\text{IP}}^{\text{a}}[\text{H}^+] + K_{\text{IP}}^{\text{b}}K_{\text{a}}^{\text{Ru}})K_{\text{a}}^{\text{Fe}}[\text{Fe}(\text{CN})_6^{4-}]/([\text{H}^+] + K_{\text{a}}^{\text{Fe}})]}{(9)}$$

of k_{obsd} were fitted to eq 9 by means of a nonlinear least-squares calculation with K_{IP}^{b} estimated at 2.0×10^2 .²⁴ We obtained $K_{\text{IP}}^{\text{a}} = (2.1 \pm 0.6) \times 10^3 \text{ M}^{-1}$ and $k = (6.9 \pm 0.7) \times 10^{-4} \text{ s}^{-1}$. Parallel studies²⁵ on the formation of III from Ru(NH₃)₅OH₂³⁺ and Ru(CN)₆⁴⁻ with [Ru(CN)₆⁴⁻] = (0.64–7.81) × 10⁻³ M and pH 4.00–5.32 yielded $K_{\text{IP}}^{\text{a}} = (1.4 \pm 0.6) \times 10^3 \text{ M}^{-1}$ and $k = (7.8 \pm 0.9) \times 10^{-4} \text{ s}^{-1}$. Equilibrium constants for ion-pair formation between M(NH₃)₅L³⁺ and M'(CN)₆⁴⁻ (M = Co, Ru; L = H₂O, pyridine, isonicotinamide, nicotinamide, 4,4'-bipyridine, 4-cyanopyridine; M' = Fe, Ru, Os)¹⁹ fall in the range (1.5–2.9) × 10³ M⁻¹, in excellent agreement with the values obtained in the present work. Although very few ligation reactions of Ru(NH₃)₅OH₂³⁺ have been studied, a value of $5 \times 10^{-4} \text{ s}^{-1}$ for the water-exchange reaction of Ru(NH₃)₅OH₂³⁺ has been estimated.¹⁷ This value is in remarkable agreement with the range of values (7–8) × 10⁻⁴ s⁻¹ for the water-ligand interchange reactions of the ion pairs Ru(NH₃)₅OH₂³⁺|M(CN)₆⁴⁻ (M = Fe, Ru) measured in the present work. The agreement, consistent with a dissociative mechanism, may be fortuitous, however, since substitution reactions of Ru(NH₃)₅OH₂³⁺ appear to be associatively activated.²⁶

The IV band of II has an energy of 10 200 cm⁻¹, a half-width of 4100 cm⁻¹ and a molar absorbance equal to $3.0 \times 10^3 \text{ M}^{-1} \text{ cm}^{-1}$. There is little doubt that II is a valence-trapped species containing Ru(III) and Fe(II). The absence of the 420-nm band in II, a band characteristic of Fe(III), has already been alluded to, and this indicates the presence of Fe(II) (and Ru(III)). Moreover, the band responds to changes in the identity of the metal as expected on the basis of a Fe(II)–Ru(III) assignment. Thus, the intervalence band in III appears at 680 nm.²⁷ The difference in the energies of the IV bands in II and III amounts to 0.56 V. This value compares very favorably with the difference in the energies of the IV bands between (NH₃)₅Os^{III}NCFe^{II}(CN)₅⁻ (628 nm) and (NH₃)₅Os^{III}NCRu^{II}(CN)₅⁻ (490 nm), namely, 0.56 V.²⁸ The energy is also in excellent agreement with the difference in the energies of the *outer-sphere* IV bands: in the Ru(NH₃)₆³⁺|Fe(CN)₆⁴⁻ (714 nm¹⁹) and Ru(NH₃)₆³⁺|Ru(CN)₆⁴⁻ (549 nm²⁹) ion

Scheme II



pairs, 0.52 V; in the Ru(NH₃)₅py³⁺|Fe(CN)₆⁴⁻ (910 nm¹⁹) and Ru(NH₃)₅py³⁺|Ru(CN)₆⁴⁻ (643 nm¹⁹) ion pairs, 0.57 V; in the EuC2.2.1³⁺|Fe(CN)₆⁴⁻ (530 nm³⁰) and EuC2.2.1³⁺|Ru(CN)₆⁴⁻ (434 nm³⁰) ion pairs, 0.52 V. The 0.52–0.57 V energy difference is also in excellent agreement with the difference in the reduction potentials between the Ru(CN)₆^{3-/4-} (0.94 V) and Fe(CN)₆^{3-/4-} (0.42 V) couples, 0.52 V, and is expected on the basis of eq 10^{31,32}

$$E_{\text{op}} = 4\Delta G^* + E_0 \quad (10)$$

provided that ΔG^* , the reorganization energy for thermal electron transfer, is similar for Fe(CN)₆⁴⁻ and Ru(CN)₆⁴⁻ and that E_0 , the free energy difference between the two oxidation state isomers of the binuclear complex or ion pair, changes in going from Fe(CN)₆⁴⁻ to Ru(CN)₆⁴⁻ by the same amount as the reduction potentials of the Fe(CN)₆^{3-/4-} and Ru(CN)₆^{3-/4-} couples. In eq 10, E_{op} is the energy of the optical transition corresponding to the IV band. The first proviso is indeed met since it has been shown²⁴ that the rate constants for the self-exchange reactions of the Fe(CN)₆^{3-/4-} and Ru(CN)₆^{3-/4-} couples are within a factor of 2 from each other. The second proviso needs some elaboration. Goldsby and Meyer³³ found that changes in E_{op} for a series of Ru–Ru and Ru–Os binuclear complexes (bpy)₂ClRuLMCl-(bpy)₂³⁺ (M = Ru, Os; L = pyrazine, 4,4'-bipyridine, 2,2'-bipyrimidine) parallel very closely the changes in the reduction potentials of the pertinent couples and presented a thermodynamic analysis showing that changes in E_0 in going from Ru to Os are equal to the changes in the reduction potentials of the corresponding Ru and Os couples. For the Fe and Ru binuclear complexes studied here, we present an alternate thermodynamic analysis that leads to the same conclusion. Consider Scheme II. Step 1 consists of the electronic isomerization and has a free energy change³⁴ E_0 . Steps 2 and 3 correspond to free energy changes associated with ligand substitution of water in M^{III}(CN)₅OH₂³⁻. It has been shown³⁵ that the equilibrium constants for the formation of a wide variety of Fe^{II}(CN)₅L³⁻ and Ru^{II}(CN)₅L³⁻ complexes are equal to each other within a factor of 2. Therefore, ΔG_2° and ΔG_3° are taken to be equal for Ru and Fe. The difference in the free energy changes for step 4 in going from Fe to Ru is equal to the difference in the reduction potentials of the Fe(CN)₆^{3-/4-} and Ru(CN)₆^{3-/4-} couples. The free energy change for step 5 corresponds to substitution of H₂O in Ru^{II}(NH₃)₅OH₂²⁺ by Fe(CN)₆³⁻ or Ru(CN)₆³⁻. In view of the similarity in the

(23) Although ion pairs are also formed between Ru(NH₃)₅OH₂³⁺/Ru(NH₃)₅OH₂²⁺ and HFe(CN)₆³⁻, we chose to neglect these. At the lowest pH utilized, only about 10% of the Fe(CN)₆⁴⁻ is protonated and the ion-pair formation constants of HFe(CN)₆³⁻ are about 10 times smaller than the constants for Fe(CN)₆⁴⁻.

(24) Haim, A. *Comments Inorg. Chem.* **1985**, *4*, 113.

(25) Dioxygen was not excluded after measurements in the presence and absence of dioxygen gave identical results. $\text{p}K_{\text{a}}$ values of protonated Ru(CN)₆⁴⁻ are not available. We assumed the same values as for Fe(CN)₆⁴⁻. Shepherd and co-workers¹¹ report $k = 0.7 \text{ s}^{-1}$ (22 °C) for the reaction Ru(NH₃)₅OH₂³⁺|Ru(CN)₆⁴⁻ → III. However, they prepared Ru(NH₃)₅OH₂³⁺ by oxidation of Ru(NH₃)₅OH₂²⁺ with dioxygen. Presumably, unreacted Ru(NH₃)₅OH₂²⁺ catalyzes the reaction by a mechanism similar to the one suggested in eq 3 and 4.

(26) Fairhurst, M. T.; Swaddle, T. W. *Inorg. Chem.* **1979**, *18*, 3241.

(27) Literature values are 675^{9,11} and 680 nm.¹⁰

(28) Vogler, A.; Osman, A. H.; Kunkely, H. *Inorg. Chem.* **1987**, *26*, 2337.

(29) Toma, H. E. *J. Chem. Soc., Dalton Trans.* **1980**, 471.

(30) Sabbatini, N.; Bonazzi, A.; Ciano, M.; Balzani, V. *J. Am. Chem. Soc.* **1984**, *106*, 4055.

(31) Hush, N. S. *Prog. Inorg. Chem.* **1967**, *8*, 275.

(32) This equation is derived under the assumption that E_0 is small compared to E_{op} .²⁴

(33) Goldsby, K. A.; Meyer, T. J. *Inorg. Chem.* **1984**, *23*, 3002.

(34) Marcus, R. A.; Sutin, N. *Comments Inorg. Chem.* **1986**, *5*, 119.

(35) Hoddenbagh, J. M. A.; Macartney, D. H. *Inorg. Chem.* **1986**, *25*, 2099.

charge, size, and basicity between $\text{Fe}(\text{CN})_6^{3-}$ and $\text{Ru}(\text{CN})_6^{3-}$, we take ΔG_5° to be very similar for Fe and Ru. Since $E_0 = \Delta G_2^\circ + \Delta G_3^\circ + \Delta G_4^\circ + \Delta G_5^\circ$ and ΔG_2° , ΔG_3° , and ΔG_5° are the same for Fe and Ru, it follows that the difference in E_0 between Fe and Ru is equal to the difference in the reduction potentials between the $\text{Fe}(\text{CN})_6^{3-/4-}$ and $\text{Ru}(\text{CN})_6^{3-/4-}$ couples, as observed experimentally.

Although the spectral characteristics of II discussed above support a trapped-valence formulation featuring Ru(III) and Fe(II), some delocalization obtains. The extent of delocalization can be assessed from a calculation of the parameters α^2 and H_{AB} , eq 11-13. Taking $\bar{\nu}_{\text{max}} = 1.02 \times 10^4 \text{ cm}^{-1}$, $d = 5.2 \text{ \AA}$ (distance

$$\alpha^2 = 4.24 \times 10^{-4} \epsilon_{\text{max}}(\Delta\bar{\nu}_{1/2})/\bar{\nu}_{\text{max}}d^2 \quad (11)$$

$$H_{AB} = \bar{\nu}_{\text{max}}\alpha \quad (12)$$

$$\Delta\bar{\nu}_{1/2} = (2310\bar{\nu}_{\text{max}})^{1/2} \quad (13)$$

between metal centers), and $\epsilon_{\text{max}} = 3.0 \times 10^3 \text{ M}^{-1} \text{ cm}^{-1}$, we calculate $\Delta\bar{\nu}_{1/2} = 4.9 \times 10^3 \text{ cm}^{-1}$, $\alpha^2 = 2.2 \times 10^{-2}$, and $H_{AB} =$

$1.5 \times 10^3 \text{ cm}^{-1}$ from eq 11-13. Results of similar calculations for analogous cyano-bridged binuclear complexes are presented in Table II. The small values of the delocalization parameter ($\alpha^2 \sim 2\%$) in all cases support the trapped valence description for the compounds. The extent of electronic coupling for cyano-bridged complexes is considerably higher ($H_{AB} = (1-2) \times 10^3 \text{ cm}^{-1}$) than values found for pyrazine-bridged complexes ($H_{AB} = (3-5) \times 10^2 \text{ cm}^{-1}$).^{33,36} Such a trend was noted before³⁷ and can reasonably be ascribed, if the coupling between sites is dominated by metal centers-bridging ligand mixing,³⁸ to a shorter bridge in CN^- and to the availability of a pair of perpendicular π^* orbitals on the bridging ligand. Alternatively, direct $\pi d-\pi d$ overlap may play a role in delocalization when the bridging ligand is cyanide.

Registry No. $\text{Ru}(\text{NH}_3)_5\text{OH}_2^{3+}$, 25590-52-7; $\text{Fe}(\text{CN})_6^{4-}$, 13408-63-4.

(36) Creutz, C. *Prog. Inorg. Chem.* **1983**, *30*, 1.

(37) Bignozzi, C. A.; Roffia, S.; Scandola, F. *J. Am. Chem. Soc.* **1985**, *107*, 1644.

(38) Richardson, D. E.; Taube, H. *J. Am. Chem. Soc.* **1983**, *105*, 40.

Contribution from the Edison Biological Laboratory,
Department of Chemistry, Brandeis University, Waltham, Massachusetts 02254

Oxidative Chemistry of Nickel Hydroporphyrins

Alan M. Stolzenberg* and Matthew T. Stershic

Received July 22, 1987

The chemical and electrochemical oxidations of nickel porphyrin, chlorin, and isobacteriochlorin complexes in the octaethyl and methyl-substituted octaethyl series were investigated in nonaqueous media. The potentials for oxidation of the complexes were determined by cyclic voltammetry in acetonitrile, methylene chloride, and dimethylformamide solutions containing TBAP as supporting electrolyte. EPR and absorption spectroscopy were used to characterize the one- and two-electron-oxidized complexes. The first oxidation of all complexes yielded nickel(II) cation radicals. Unlike $\text{Ni}(\text{TPP})^{2+}$, the cation radical complexes did not undergo internal electron transfer to afford nickel(III) complexes at low temperatures. Nickel(II) dication complexes were the product of the second oxidation of nickel porphyrins and chlorins in acetonitrile. The second oxidation of nickel isobacteriochlorins afforded nickel(III) cation radical complexes. The results suggest that the greatly enhanced stability of oxidized *cis*-Ni(OEC) species is not a consequence of redox activity of the coordinated nickel but rather of the ruffled conformation of the macrocycle.

Recently, we reported a remarkable increase in the stability of oxidized *cis*-octaethylchlorin species when coordinated to nickel.¹ Dications of β -hydrogenated hydroporphyrins,² of which chlorins are a subgroup, typically undergo partial dehydrogenation on the cyclic voltammetric time scale to afford more extensively unsaturated macrocycles.³ The compounds formed upon oxidation of free-base *cis*- $\text{H}_2(\text{OEC})^4$ were considerably less stable. On the same time scale, dehydrogenation of *cis*- $\text{H}_2(\text{OEC})^{2+}$ was complete and that of *cis*- $\text{H}_2(\text{OEC})^{+}$ was extensive.^{1,5} Metalation of *cis*-OEC with Cu(II), Mg(II), Sn(IV), or Zn(II) increased the stability of the cation radical somewhat, but formation of the cation radical was reversible only for the Mg complex. The second

oxidations of all four complexes remained totally irreversible. In contrast, both oxidations of *cis*-Ni(OEC) were reversible on the cyclic voltammetric time scale (100 mV/s sweep rate).

Nickel hydroporphyrin complexes differ substantially from free-base and other metallohydroporphyrin complexes in one important respect that may enhance the stability of *cis*-Ni(OEC)⁺. X-ray structural studies show that the macrocycle in nickel hydroporphyrin complexes invariably experiences a marked S_4 ruffle and is saddle-shaped.^{6,7} Ruffling is a consequence of both the flexibility of hydroporphyrins^{1,6b,7c,8} and the mismatch of the metal-nitrogen bond lengths optimal for square-planar, low-spin nickel(II) and for planar porphyrin or hydroporphyrin macrocycles.^{6b,7c} The conformations of Ni(OEC) complexes are also ruffled in solution.¹ The OEC macrocycle must therefore flatten out to form Ni(OEP) by dehydrogenation of the *cis*-Ni(OEC) dication. A comparable conformational change is not required for the dehydrogenation of the other *cis*-OEC complexes. Because ruffling of nickel hydroporphyrins is a spontaneous process, flattening the macrocycle provides an endergonic contribution to

(1) Stolzenberg, A. M.; Stershic, M. T. *Inorg. Chem.* **1987**, *26*, 1970.

(2) (a) Scheer, H. In *The Porphyrins*; Dolphin, D., Ed.; Academic: New York, 1978; Vol. 2, pp 1-44. (b) Scheer, H.; Inhoffen, H. H. *Ibid.*; pp 45-90.

(3) Stolzenberg, A. M.; Spreer, L. O.; Holm, R. H. *J. Am. Chem. Soc.* **1980**, *102*, 364.

(4) Abbreviations: OEP, 2,3,7,8,12,13,17,18-octaethylporphyrin dianion; OEC, 2,3-dihydro-2,3,7,8,12,13,17,18-octaethylporphyrin dianion (chlorin); OEiBC, mixture of *iii*- and *tet*-2,3,7,8-tetrahydro-2,3,7,8,12,13,17,18-octaethylporphyrin dianion (isobacteriochlorin); MOEC, 2,3-dihydro-2-methyl-3,3,7,8,12,13,17,18-octaethylporphyrin dianion; DMOEiBC, mixture of *syn*- and *anti*-2,7-dihydro-2,7-dimethyl-3,3,7,8,12,13,17,18-octaethylporphyrin dianion; TPP, 5,10,15,20-tetraphenylporphyrin dianion; TPC, 2,3-dihydro-5,10,15,20-tetraphenylporphyrin dianion; TPiBC, 2,3,7,8-tetrahydro-5,10,15,20-tetraphenylporphyrin dianion; DMF, *N,N*-dimethylformamide; TEAP, tetraethylammonium perchlorate; TBAP, tetra-*n*-butylammonium perchlorate; TBAH, tetra-*n*-butylammonium hexafluorophosphate.

(5) Dehydrogenation of the cation radical can occur via the thermodynamically unfavorable disproportionation to the dication, provided that the latter reacts irreversibly and rapidly. $\text{H}_2(\text{OEiBC})^{+}$ dehydrogenates in this manner, albeit more slowly.³

(6) (a) Kratky, C.; Angst, C.; Johansen, J. E. *Angew. Chem., Int. Ed. Engl.* **1981**, *20*, 211. (b) Kratky, C.; Waditschatka, R.; Angst, C.; Johansen, J. E.; Plaquevent, J. C.; Schreiber, J.; Eschenmoser, A. *Helv. Chim. Acta* **1985**, *68*, 1312. (c) Waditschatka, R.; Kratky, C.; Jaun, B.; Heinzer, J.; Eschenmoser, A. *J. Chem. Soc., Chem. Commun.* **1985**, 1604.

(7) (a) Ulman, A.; Fisher, D.; Ibers, J. A. *J. Heterocycl. Chem.* **1982**, *19*, 409. (b) Gallucci, J. C.; Sweptson, P. N.; Ibers, J. A. *Acta Crystallogr., Sect. B: Struct. Crystallogr. Cryst. Chem.* **1982**, *B38*, 2134. (c) Suh, M. P.; Sweptson, P. N.; Ibers, J. A. *J. Am. Chem. Soc.* **1984**, *106*, 5164.

(8) (a) Strauss, S. H.; Silver, M. E.; Ibers, J. A. *J. Am. Chem. Soc.* **1983**, *105*, 4108. (b) Strauss, S. H.; Silver, M. E.; Long, K. M.; Thompson, R. G.; Hudgens, R. A.; Spartalian, K.; Ibers, J. A. *J. Am. Chem. Soc.* **1985**, *107*, 4207.